

2015

Benchmarking of Computational Models against Experimental Data for Velocity Profile Effects on CFD Analysis of Adiabatic Film-Cooling Effectiveness for Large Spacing Compound Angle Full Coverage Film Cooling Arrays

Simon Martinez
martis19@my.erau.edu

Follow this and additional works at: <https://commons.erau.edu/mcnair>

Recommended Citation

Martinez, Simon (2015) "Benchmarking of Computational Models against Experimental Data for Velocity Profile Effects on CFD Analysis of Adiabatic Film-Cooling Effectiveness for Large Spacing Compound Angle Full Coverage Film Cooling Arrays," *McNair Scholars Research Journal*: Vol. 2 , Article 1.
Available at: <https://commons.erau.edu/mcnair/vol2/iss1/1>

This Article is brought to you for free and open access by the Journals at Scholarly Commons. It has been accepted for inclusion in McNair Scholars Research Journal by an authorized administrator of Scholarly Commons. For more information, please contact commons@erau.edu.

Benchmarking of Computational Models against Experimental Data for Velocity Profile Effects on CFD Analysis of Adiabatic Film-Cooling Effectiveness for Large Spacing Compound Angle Full Coverage Film Cooling Arrays

Author: Simon R. Martinez

Mentor: Professor Timothy Smith

Embry Riddle Aeronautical University

Spring 2015

Embry-Riddle Aeronautical University

Abstract

This study aims to benchmark experimental data that tested the effects of blowing ratio, surface angle, and hole spacing for full coverage geometries composed of cylindrical staggered holes at a compounded angle of 45 degrees. These holes had an inclination angle of 45 degrees, while maintaining a lateral and axial spacing of 14.5 hole diameters. Within this study, the local film cooling effectiveness was obtained from 30 rows for the 14.5 diameter spacing. The goal of this research was to test the effects of utilizing a realistic vs a uniform velocity profile at the crossflow inlet and find any significant differences in the results produced when compared to experimental data. The results displayed differences between the spanwise average adiabatic effectiveness for both the uniform velocity profile case and the velocity profile replication of the experimental data when using the Realizable $k-\epsilon$ turbulence model. These differences were found to be due to the differences in the thermal boundary layer predicted by the turbulence model for the two test cases.

1 Introduction

Film cooling is characterized by the use of ejecting coolant at discrete locations along a surface that is exposed to a high temperature environment. The goal for this ejected coolant is to provide a thermal blanket that protects the surface from the surrounding extreme temperatures both locally at the injection location as well as downstream.

Ever since the infancy of turbine blade film cooling during the 1970's, researchers and engineers quickly found out there was large efficiency boosting rewards within this field (Bogard, 2006). However, with the discovery of great potential in this field also came the quick understanding that there was an even greater complexity that needed to be understood before taking full advantage of these rewards. For this reason there have been thousands of research articles written over the past several decades aiming to understand more about every possible aspect of this promising technology. These studies have been on the effects of cooling in regards to turbulence intensity of the main flow, freestream boundary layer thickness, density ratio between free stream and coolant stream, momentum flux ratio, mass flux ratio, blow ratio, hole roughness, hole shape, hole blockage, hole manufacturing techniques, hole inclination angle, hole compound angle, hole length, hole spacing, hole inlet conditions, adverse pressure gradients, being -downstream of a rotating wake, hole exit shaping, hole embedded in trenches, film jet Mach number, various Reynolds numbers, etc. Due to the vast amount of research articles available concerning the film cooling subject, only studies of direct importance will be presented in this work.

This current work is defined by several objectives all aimed to provide a better understanding of film cooling prediction capabilities using commercially available tools. Computational fluid dynamics (CFD), since its infancy, has been a very useful tool for engineers

to provide predictions of flow characteristics within various applications. However CFD, although a widely used tool, cannot be fully trusted with today's computational methods, which forces companies to spend extra money for corresponding experimental and operational test data. If CFD can gain a greater trustworthiness for its results, it would allow engineers to have greater accuracy of what the final design should be within the preliminary phase. This will reduce the amount of iterations a company needs to have going from the preliminary design phase to the build and test phases. For this reason, comes the need to benchmark against experimental data the various CFD parameters that could cause variation in the solutions. These parameters in question that must be tested in order to provide a reliable computational analysis include but are not limited to mesh size, domain simplifications, turbulence models, and boundary conditions. Once benchmarked, CFD has the capability of providing to the designer the ability to gather various parameter data at specific locations within the test set up with a level of detail that would be very difficult to gather experimentally. This will allow the designer to make accurate adjustments to key areas within the component to create the desired effect.

Within this current work, the experimental data that the CFD will be benchmarked against is that gathered from the University of Central Florida (Natsui, 2012). The CFD software used will be STAR-CCM+ 9.02.007 created by CD-Adapco.

With a thorough understanding of how the various geometries tested experimentally at the University of Central Florida compare to the numerical solution provided by CFD, this study intends to make some conclusions on the effects of implementing a realistic velocity profile inlet rather than a uniform velocity profile inlet. When benchmarked against experimental data, the outcome of this research will provide additional knowledge concerning implementing boundary conditions for accurate CFD modeling of adiabatic effectiveness for large spacing compound angle full coverage film cooling arrays.

2 Computational Domain and Modeling

In this current work, a computational domain was created to accurately represent the FCA geometry used in the experimental study done by Natsui (Natsui, 2010). This included the plenum, exit into the atmosphere, as well as all aerodynamic parameters found in the experimental study.

Because the experimental geometry size was so large with a length and width of 1.2m and 0.55m respectively and the need to have detailed analysis of the film holes that were 2.5mm in diameter, it became important to find ways to reduce the computational cost of the analysis without losing accuracy. For this reason, since the geometry was symmetrical along the stream wise direction, the geometry was divided in half and tested to verify that no change in the numerical solution occurred. The test results can be seen in Figure 1 which displays how no visual changes occurred in the results of adiabatic effectiveness when dividing the symmetrical geometry in half and using the Realizable k- ϵ turbulence model. The results of no change in the solution after dividing the geometry in half was expected since it has been done before in past experiments from the literature (El-Gabry & Kaminski, 2005).

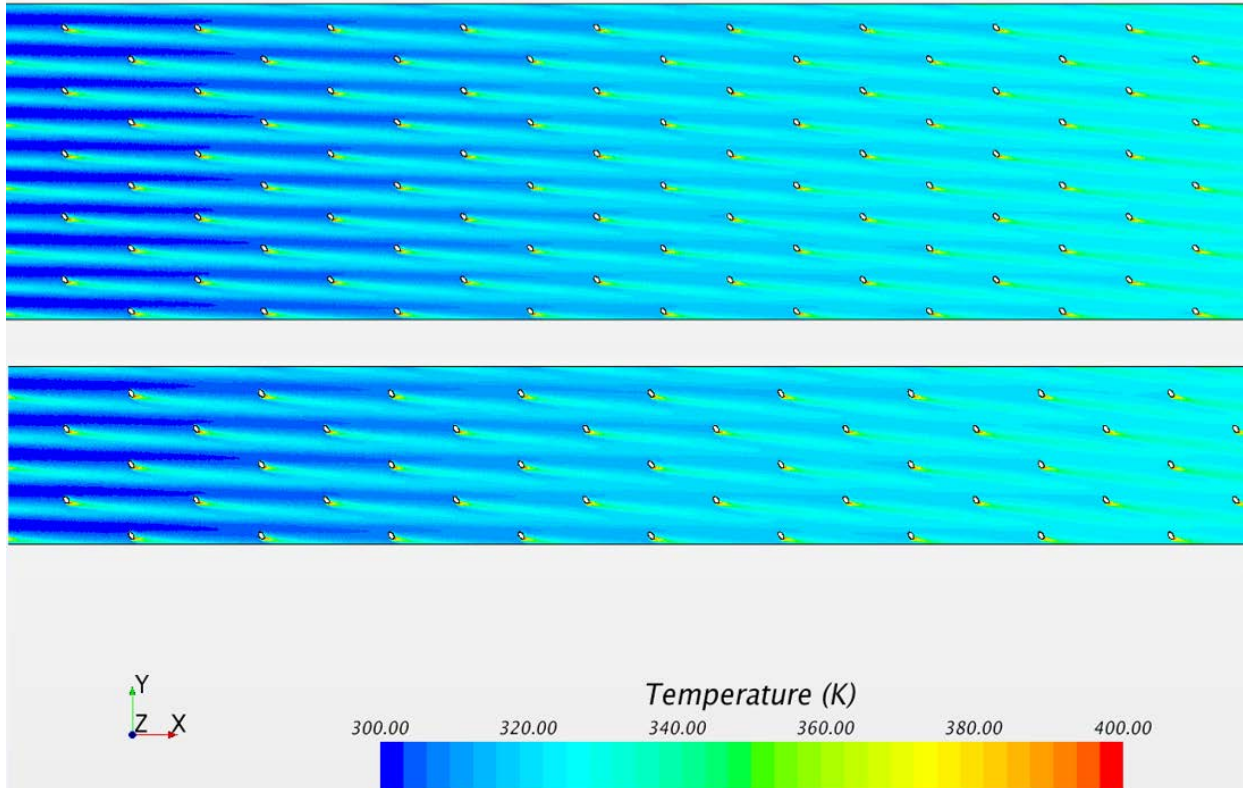


Figure 1: Domain Numerical Comparison of Cutting Geometry in Half

Once it was verified that cutting the domain in half would not change the solution, a mesh independent study was conducted. As can be seen in Table 1 and Figure 2, the surface average temperature returned from the computer simulation began to level off between a cell count of 16 million to 58 million with the range between the values being returned with a difference of only 0.2 degrees K or 0.063%. From the visual seen in Figure 2 of the change in surface average temperature as a function of cell count, initially it was decided to use a mesh size with a cell count of 36 million, which was fine enough to provide a converged solution that captured the flow phenomena. A visual of how the final geometry with this cell count looked can be seen in Figure 3, Figure 4, and Figure 5. Variation in fineness and coarseness of the mesh was implemented at different locations of the mesh to be computationally efficient as well as to maintain accuracy within key locations. As can be seen in Figures 4 and Figure 5, approximately 40 cells were used to cover the hole diameter D (2.5 mm) at the adiabatic wall in order to capture the flow phenomenon at this location because higher accuracy is desired here and higher variation of values is expected at this location. This is different than what is expected further away from the film jet holes as can be seen in Figure 3, which is why approximately 100 cells were used to capture flow within a $60D$ height within the cross flow inlet, cross flow outlet, and the overall air duct.

Table 1: Mesh Independent Study Values Gathered

Cell Count (millions)	Surface Average Temperature (K)	Percent Change In Surface Average Temperature
58	318.1	0.0313 %
36	318.0	0.0313 %
24	318.1	0.0314 %
16	318.2	0.25 %
10	319	N/A

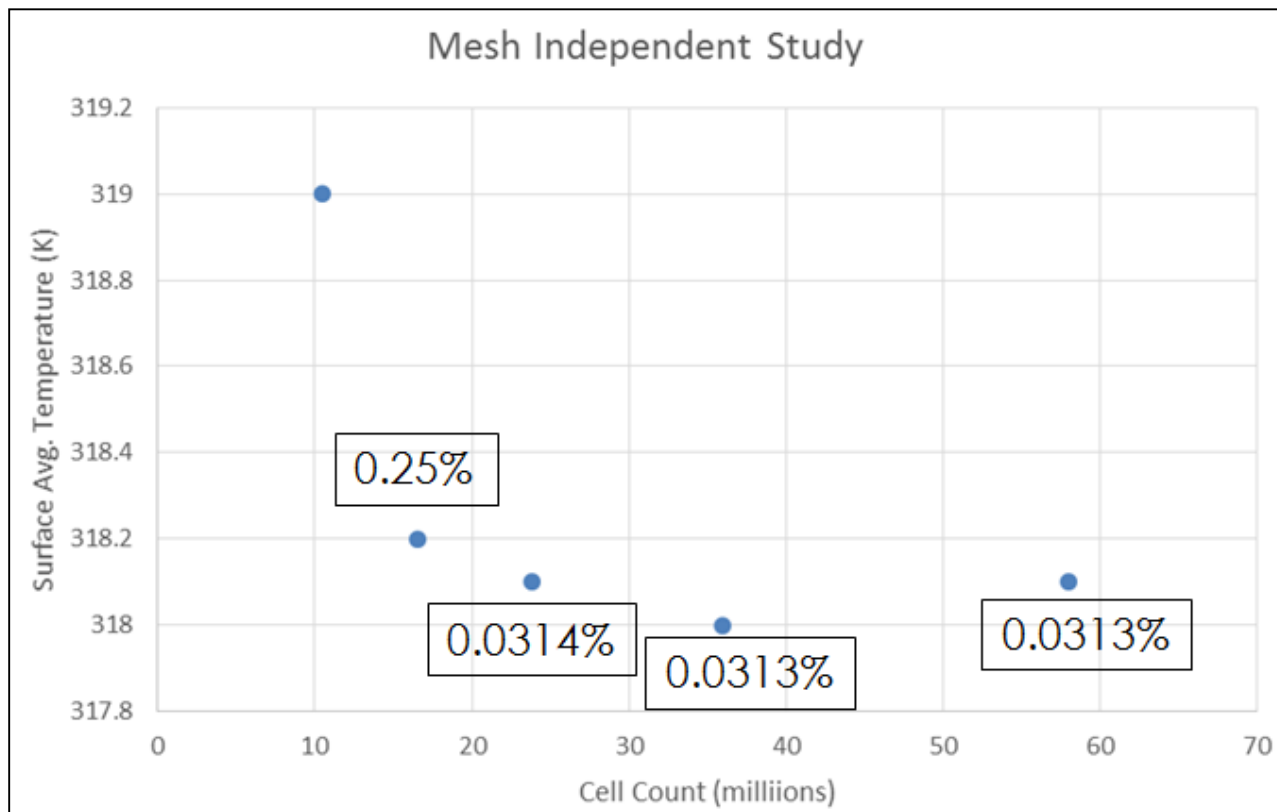


Figure 2: Mesh Independent Study

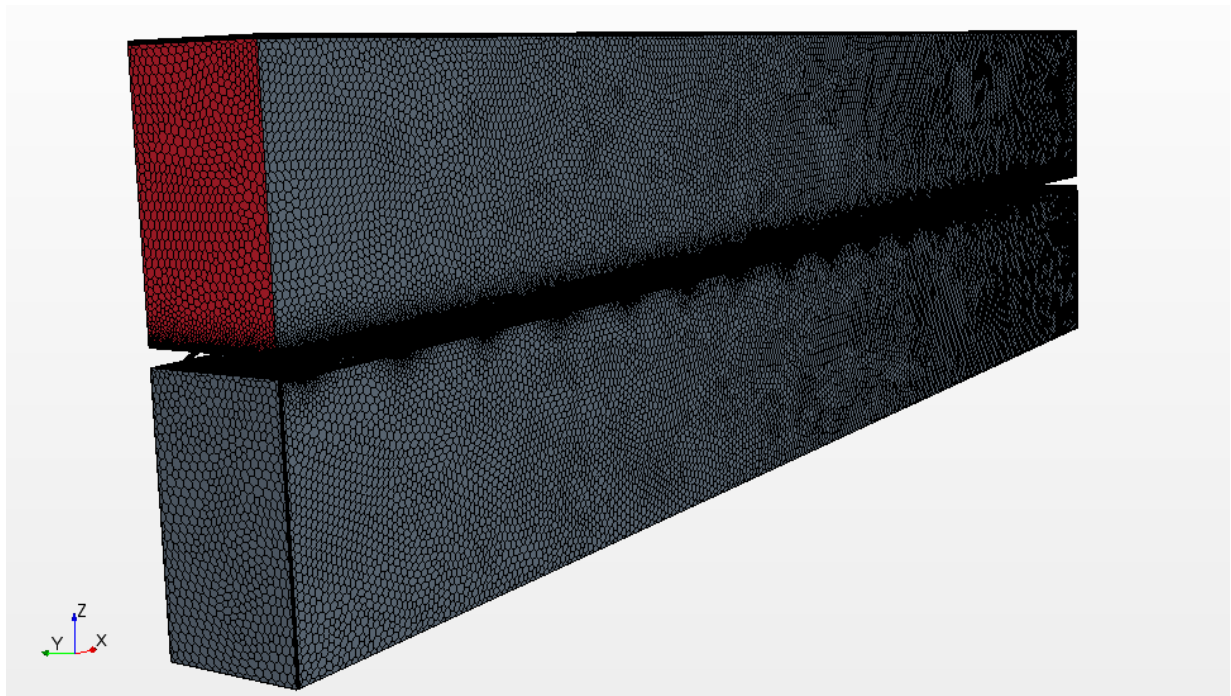


Figure 3: Full Mesh Geometry

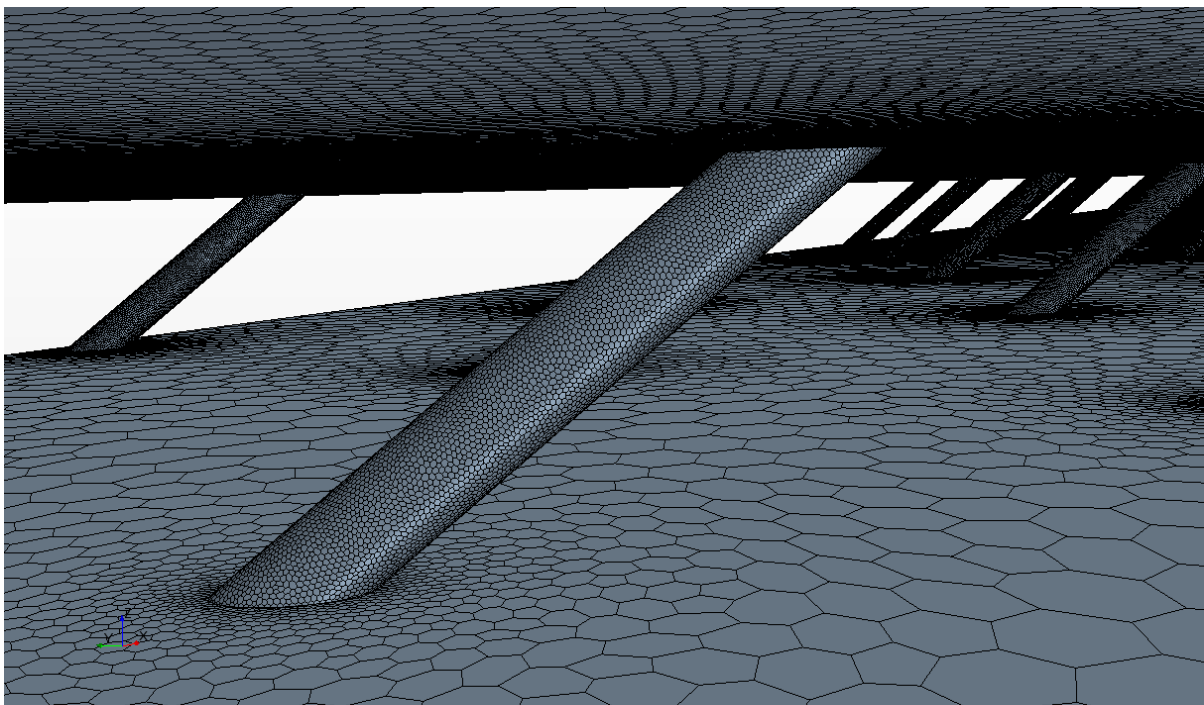


Figure 4: Close up View of Mesh at Film Hole Locations

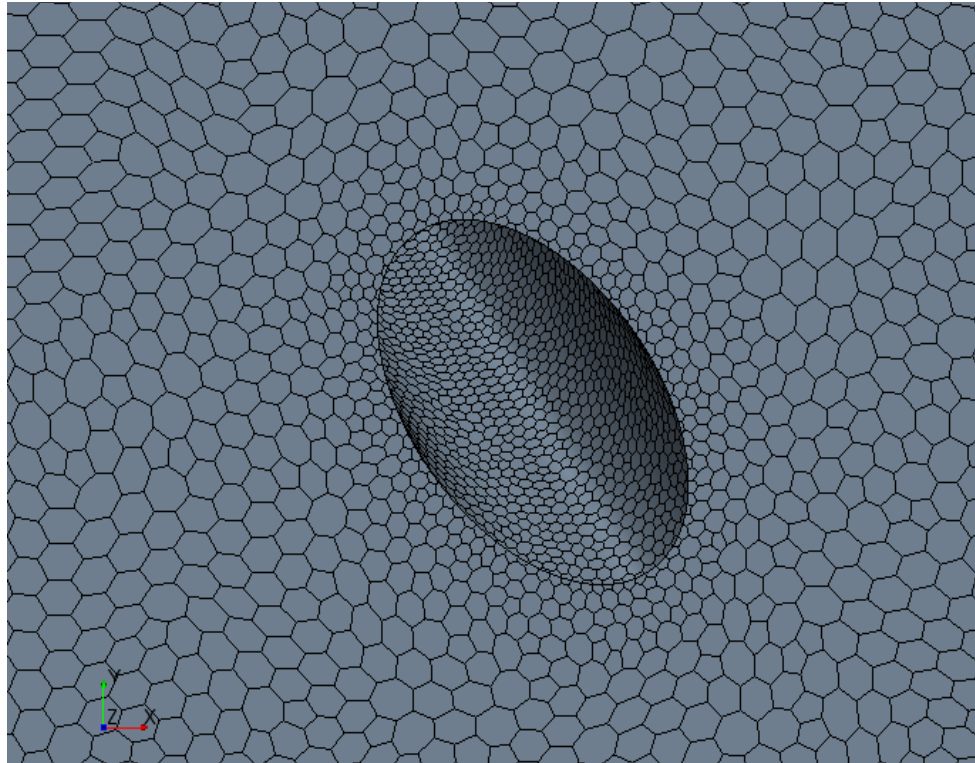


Figure 5: Close-Up Top View of Film Hole Outlet

In order to ensure the capture of the heat transfer and fluid effects near the wall of the adiabatic test section, the all y^+ wall treatment was set to be less than 1 throughout the region as can be seen in Figure 6. The reason for this all y^+ wall treatment is so that the near-wall cells within the boundary layer region can properly produce accurate results. This y^+ wall treatment allows the simulation to properly connect the viscosity affected boundary layer region near the wall with the fully turbulent region, which is then calculated through the use of turbulence models.

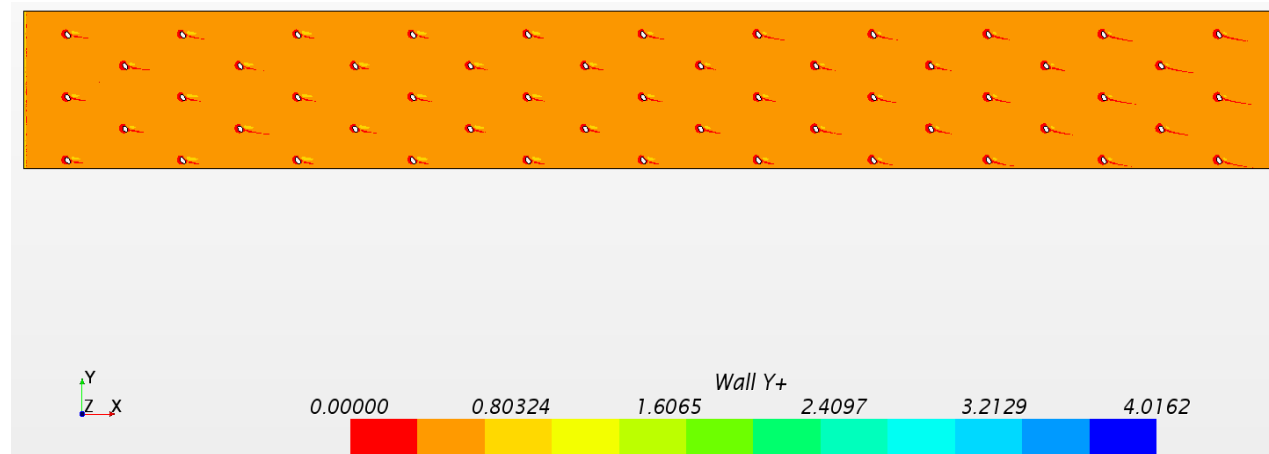


Figure 6: All Y^+ Wall Treatment Less Than One on Adiabatic Test Surface

Near the adiabatic wall test section, in the aim to both capture the presence of the boundary layer near the wall as well as save computational cost, 15 prism layers were used with a 20% increase in size per layer. This allowed a fine enough mesh distribution to be present near the wall region where the boundary layer is expected to be. Figure 7 gives a visual representation of the prism layers used within the geometry.

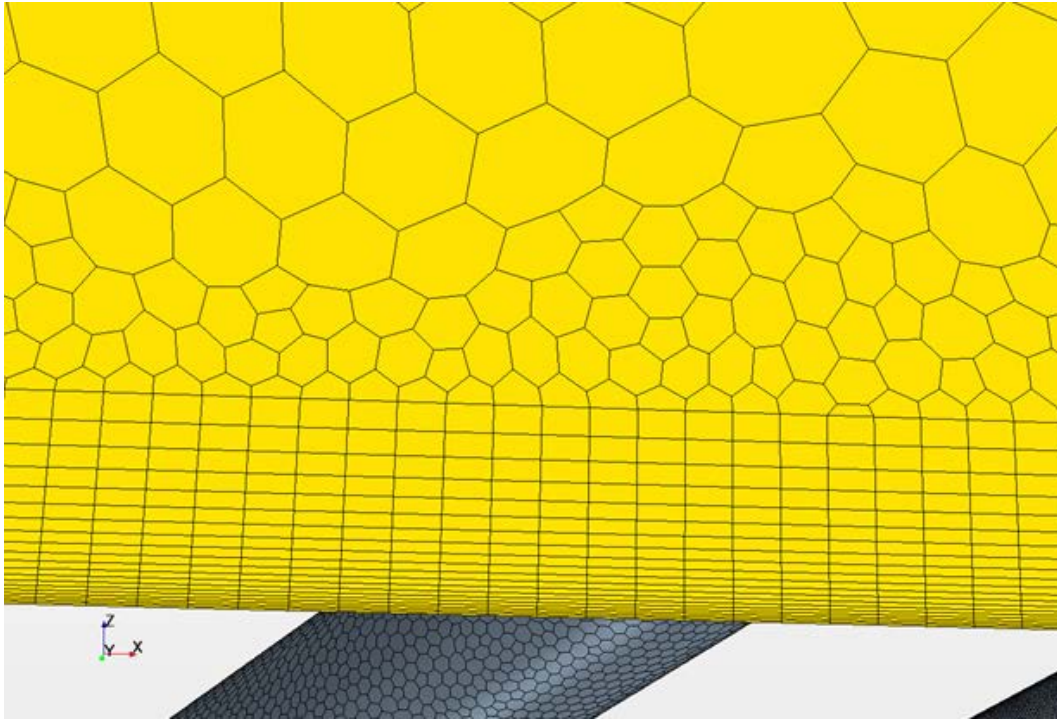


Figure 7: Prism Layers Used Near Adiabatic Wall Location

The boundary conditions for the CFD simulation using Star-CCM+ was set to replicate the same boundary conditions found in the experimental testing done by Natsui for the FCA geometry.

As for various key areas within the geometry such as the cross flow inlet, plenum inlet, cross flow outlet, adiabatic wall, and film holes, the boundary conditions placed for each of these locations can be seen in Figures 8 and 9 as well as Table 3. For the cross flow inlet, the temperature was set at 300K while the plenum inlet (coolant location) was set at 400K. In order to mimic the experimental data's blowing ratio of $M=0.4$ for the CFD simulation, the mass flow within the plenum inlet was set to be 0.004679 kg/s, as can be seen in Table 2.

Table 2: Mass Flow Variation Per Geometry

Blowing Ratio	Geometry	Mass Flow (kg/s)
0.4	FC.A	0.004679

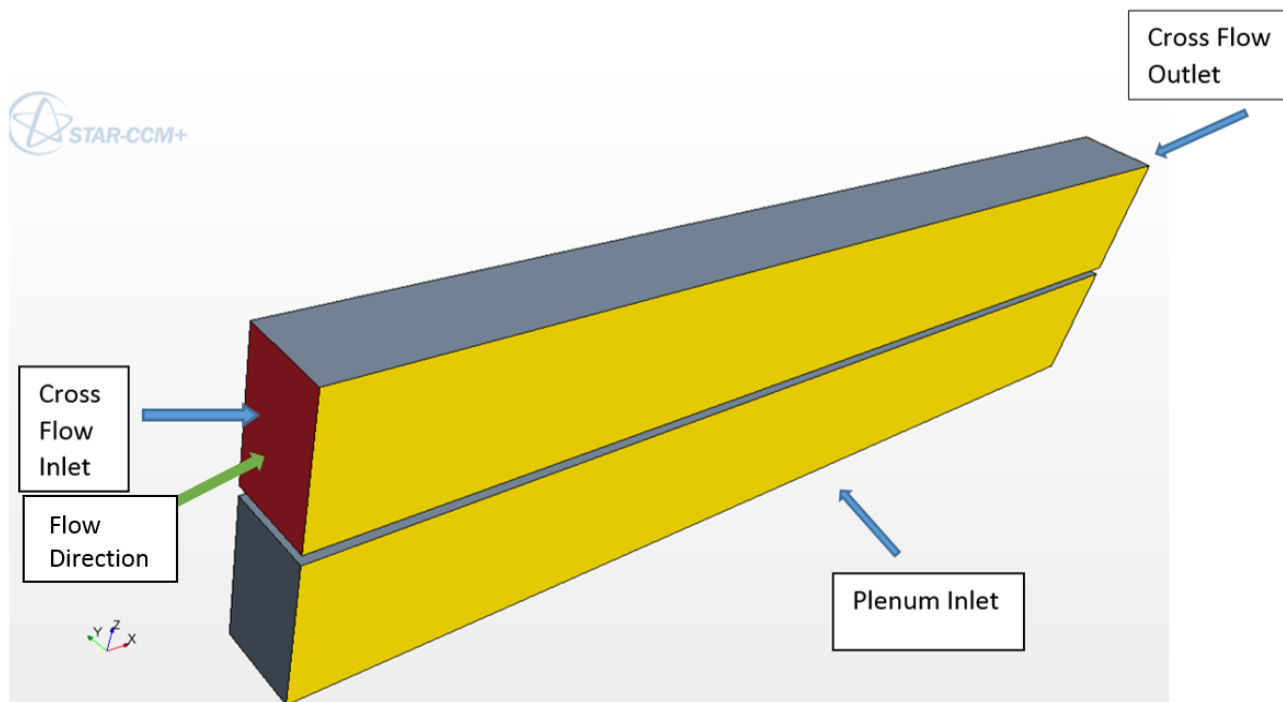


Figure 8: Far View of Boundary Condition Locations

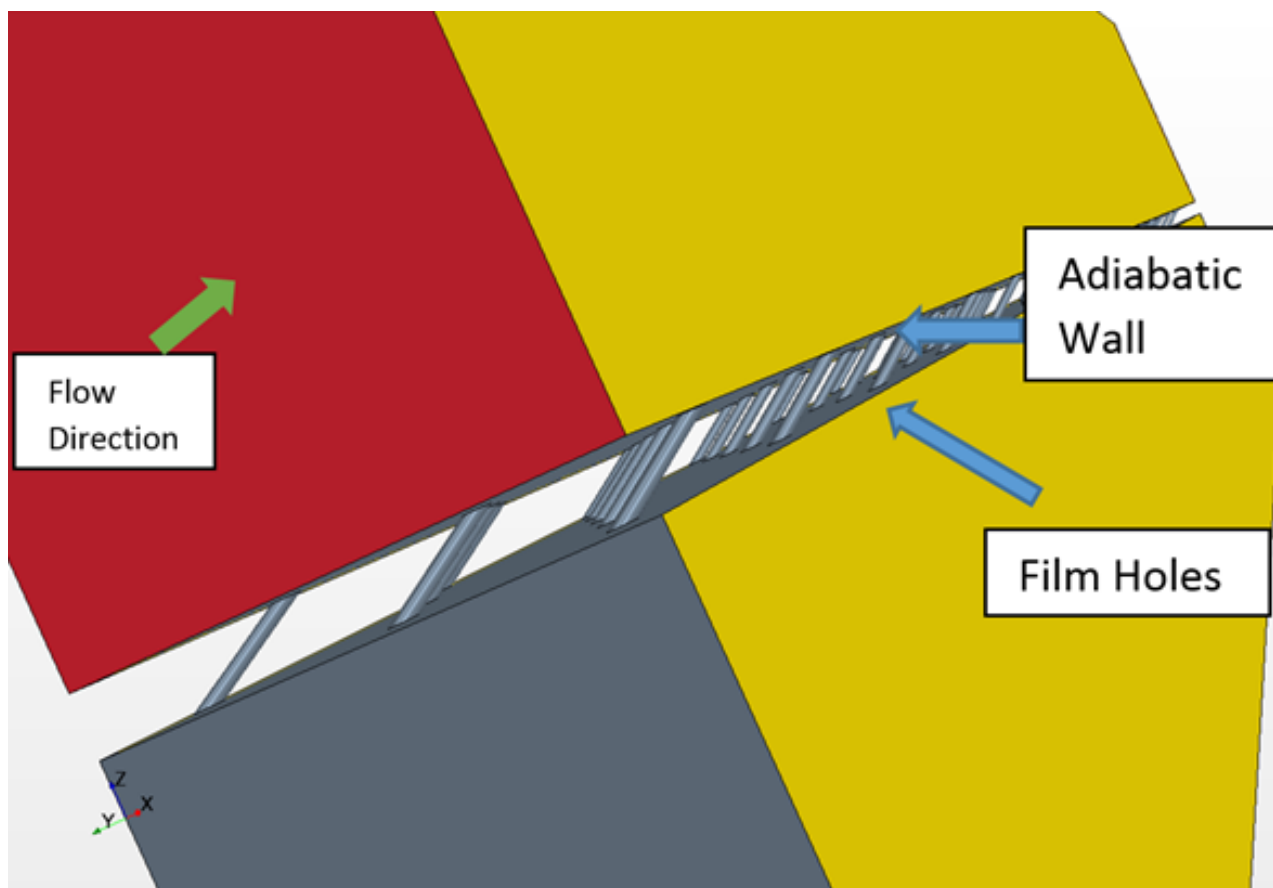


Figure 9: Close-Up View of Boundary Condition Locations

Table 3: Boundary Conditions Used Per Domain Section

Section	Boundary Conditions
Cross Flow Inlet	Velocity Profile
Cross Flow Outlet	Pressure Outlet
Plenum Inlet	Mass Flow Inlet
Adiabatic Wall	Adiabatic-, No-Slip Condition

3 Velocity Profile Effects

The boundary conditions regarding the velocity profile were tested within this study using the realizable $k-\epsilon$ turbulence model. The reason for using this turbulence model is because past research has shown accuracy and reliability of this turbulence model for similar full coverage film cooling geometries in the past (Natsui, 2010). For this reason, the realizable $k-\epsilon$ turbulence model was found suitable as the initial turbulence model to use for the study of the effects of implementing a velocity profile. Although the CFD software allows for a uniform velocity inlet profile, with the motivation to replicate the experimental data as much as possible, the effects of including the velocity profile witnessed during the experiment were tested. Using the velocity profile data found within the experimental study (Natsui, 2012), the velocity profile displayed in Figure 10 was implemented as a boundary condition within the cross flow inlet location in the CFD simulation. As for the uniform velocity profile test case, a uniform velocity of 27m/s was used, which was the expected velocity of the flow far away from the wall. Once this velocity profile was used, it was shown that there were some distinct differences gained within the analysis when compared to the experimental data. As can be seen in Figure 11-, from the location of film hole rows 1-6-, there is nearly no difference between the effects of using a velocity profile vs not using a velocity profile. This can be attributed to the turbulence model used (Realizable $k-\epsilon$) within this velocity profile comparison's capability to replicate the same thermal boundary layer for these two cases for rows 1-6, which can be seen in Figure 12. However, for the locations downstream at rows 7-16 the velocity profile case's thermal boundary layer becomes more pronounced sooner than the non-velocity profile case as can be seen in Figure 12. This causes an increase in spanwise average adiabatic effectiveness for the case with the velocity profile as opposed to the non-velocity profile case for rows 7-16, which can be seen in Figure 11. For the remainder of the rows 16-30, adiabatic effectiveness is shown to be higher for the non-velocity profile case as can be seen in Figure 11. This higher result for adiabatic effectiveness for the non-velocity profile case within far downstream locations was found to be due to the more pronounced thermal boundary layer produced from the simulation as can be seen in Figure 13. Because a thermally cooler environment was produced due to the greater thermal boundary layer cooling effect of the non-velocity profile case, it resulted in providing a surface temperature cooler than that of the velocity profile case which resulted in a higher adiabatic effectiveness value at these downstream locations.

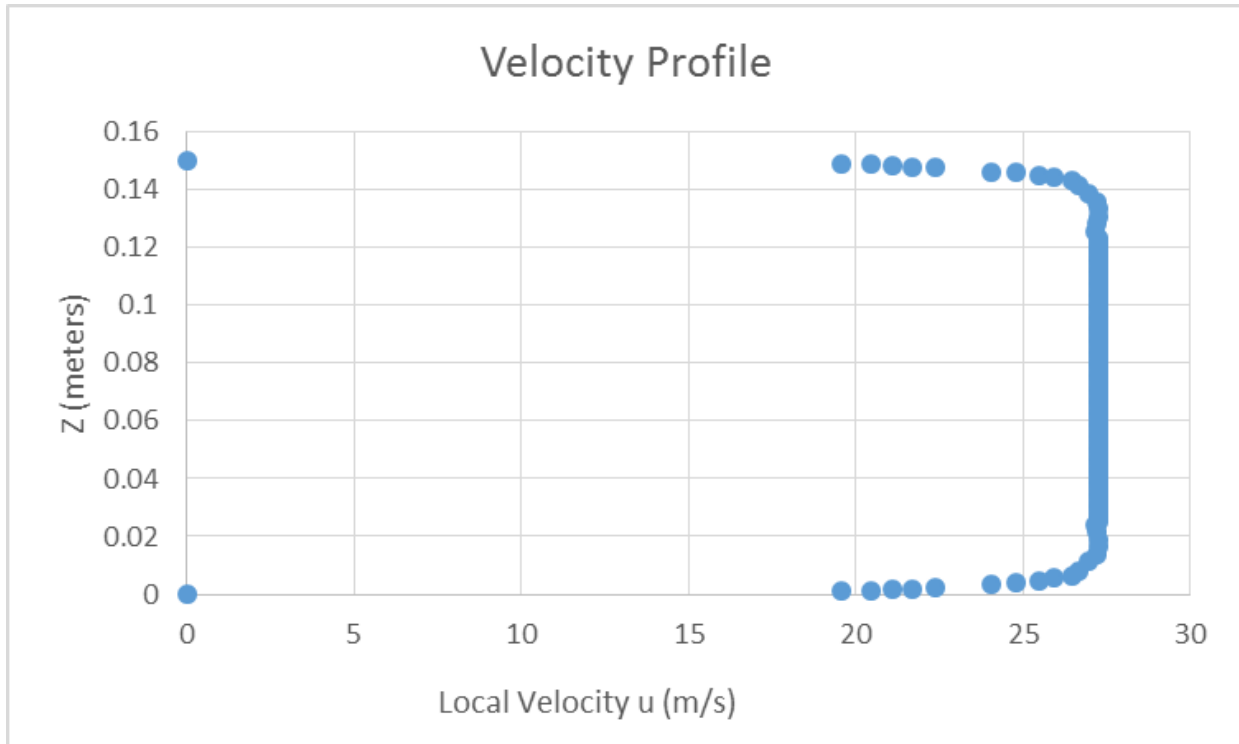


Figure 10: Velocity Profile Used Within CFD Simulation

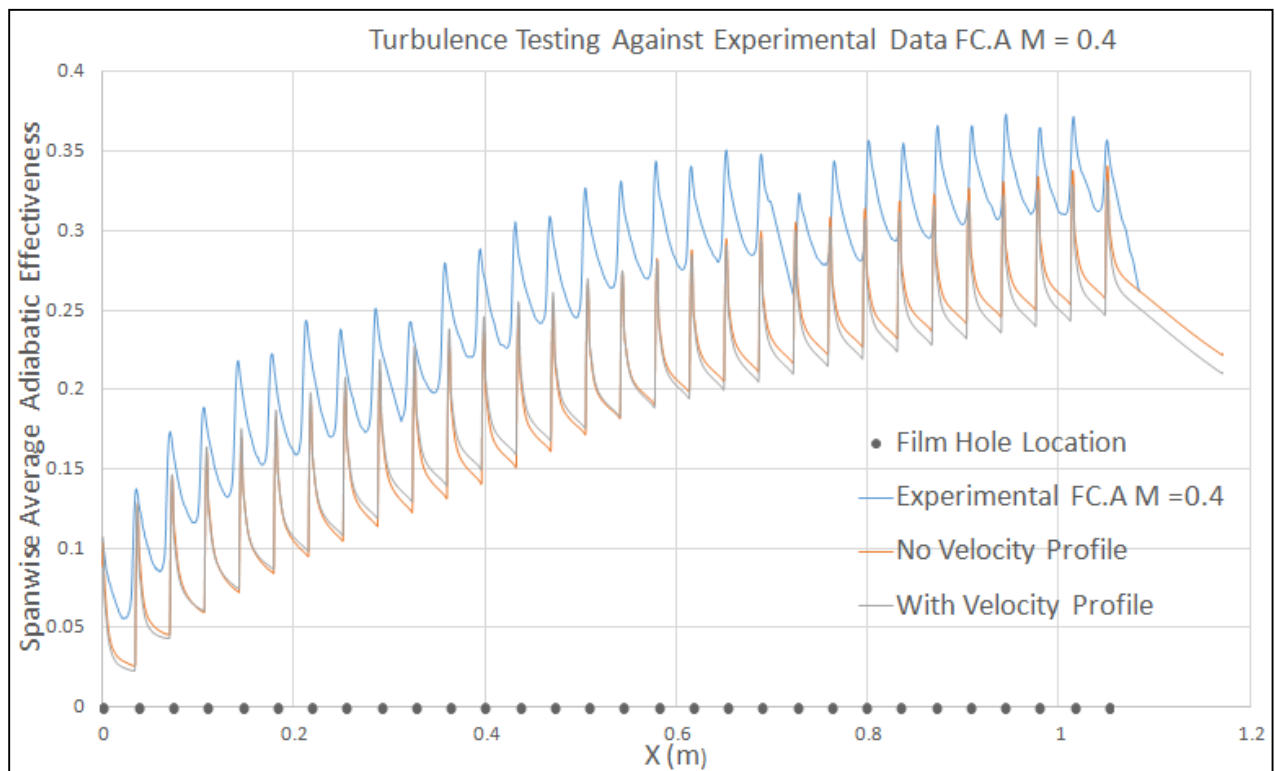


Figure 11: Effects of Using Velocity Profile Vs Not Using a Velocity Profile

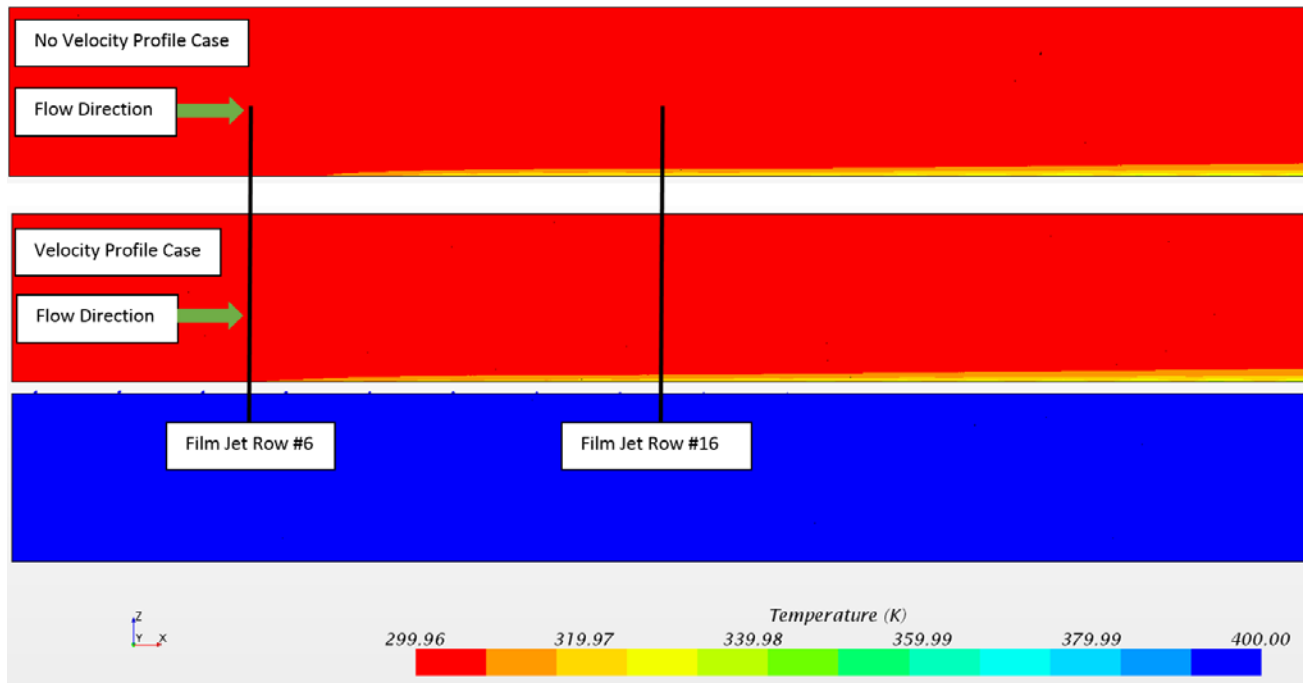


Figure 12: Effects of Velocity Profile on Thermal Boundary Layer Upstream

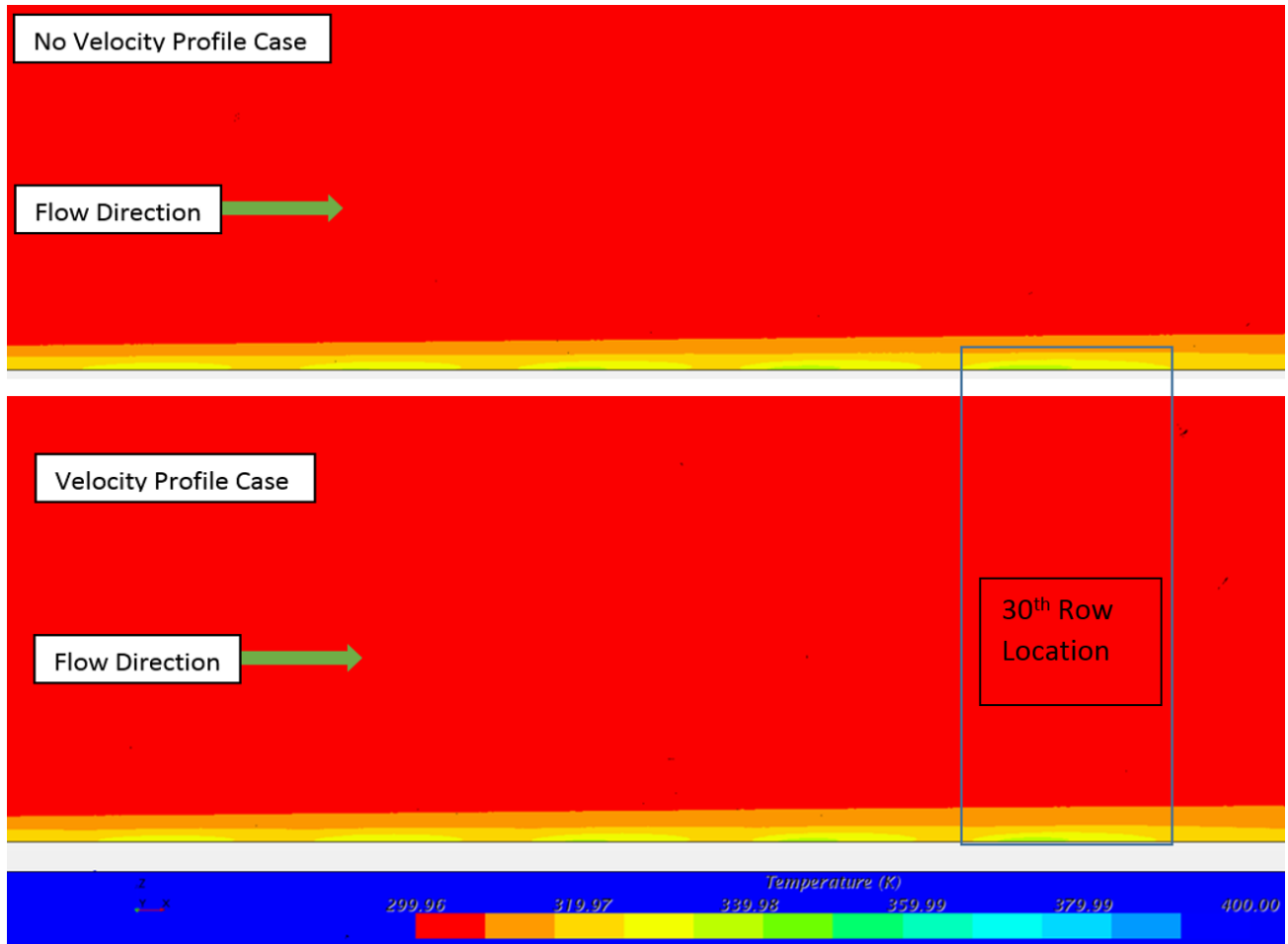


Figure 13: Effects of Velocity Profile on Thermal Boundary Layer Downstream

4 Conclusion

The overall results of this study showed that the CFD simulations will display differences in adiabatic effectiveness values produced whether a velocity profile or a uniform flow is used. For this reason, it is important to take the effects of using a realistic velocity profile into consideration when trying to simulate a real experiment.

References

Bogard, D. G. (2006). Gas Turbine Film Cooling. *Journal Of Propulsion And Power*.

El-Gabry, L., & Kaminski, D. (2005). Numerical Investigation of Jet Impingement with Cross Flow- Comparison of Yang-Shih and Standard k-e Turbulence Models. *Journal of Numerical Heat Transfer*.

Natsui, G. (2012). Experimental Evaluation of Large Spacing Compound Angle Full-Coverage Film Cooling Arrays: Adiabatic Film Cooling Effectiveness. *ASME Summer Heat Transfer Conference HT2012-58131*.

Natsui, G. (2010). Surface Measurements and Predictions of Full-Coverage Film Cooling.